

Sub-pixel Methods for Improving Vector Quality in Echo PIV Flow Imaging Technology

Lili Niu, Jing Wang, Ming Qian and Hairong Zheng*, *Member, IEEE*

Abstract—Developments of many cardiovascular problems have been shown to have a close relationship with arterial flow conditions. An ultrasound-based particle image velocimetry technique (Echo PIV) was recently developed to measure multi-component velocity vectors and local shear rates in arteries and opaque fluid flows by identifying and tracking flow tracers (ultrasound contrast microbubbles) within these flow fields. To improve the measurement accuracy, sub-pixel calculation method was adopted in this paper to maximize the ultrasound RF signal and B mode image correlation accuracy and increase the image spatial resolution. This algorithm is employed in processing both computer-generated particle image patterns and the B-mode images of microbubbles in rotating flows obtained by a high frame rate (up to 1000 frames per second) ultrasound imaging system. The results show the correlation of particle patterns and individual flow vector quality are improved and the overall flow mappings are also improved significantly. This would help the Echo PIV system to provide better multi-component velocity accuracy.

I. INTRODUCTION

Developments of many cardiovascular problems such as atheroma, intimal hyperplasia, thrombus and hemolysis have been shown to have a close relationship with arterial flow conditions [1-3]. In particular, fluid shear stress is considered an important mediator in the development of the above problems. Thus, accurate measurement of fluid shear stress in arteries is essential both as a prognostic aid and for following disease and treatment progression. For example, shear force has long been implicated in the initiation and localization of atherosclerosis, a leading cause of morbidity and mortality in the developed world [4]. Many *in vitro* and *in vivo* studies found that the magnitude and rate of change of shear stress nearby vessel wall are linked to the pathogenesis of atherosclerosis [5-8]. Recent molecular and cellular level studies found that

hemodynamic shear gradient stimulates the endothelial cell proliferation and favors atherosclerosis development [9-11]. Therefore, wall shear stress mapping becomes an important part of the multifactorial, multidisciplinary approach to early atherosclerosis detection [4, 5, 12]. Similarly, from a biomechanical point of view, abdominal aortic aneurysms (AAAs) rupture risk is probably more precisely related to certain mechanical factors, such as flow fields, velocity patterns and flow-induced wall stresses [13-16]. The internal stress within the lesion wall develops as a result of blood flow through the vessel, since flowing blood exerts both normal and shear forces on the wall inner surface and these forces are transmitted into the wall interior. As a result, the magnitude and distribution of wall stresses are determined in part by luminal flow properties, as well as by bulge shape and diameter and wall material properties [17].

For accurate *in vivo* measurement of velocity vectors and shear stress, magnetic resonance imaging (MRI) and ultrasound Doppler techniques have been investigated; however, both have limitations [4, 5]. Conventional Doppler has the problem of angulation error, which limits the measurement to only the component of velocity along the ultrasound beam, thus requiring parallel alignment of the ultrasound beam to the flow direction. MRI is an attractive technique for blood velocity measurements since it provides multiple components of blood flow and has high spatial resolution. However, MRI possesses several limitations such as its cumbersome nature, expense in time and costs, and poor temporal resolution. Thus, a non-invasive technique with good temporal and spatial resolution that can measure multiple velocity vectors (and thereby local shear stress) in real time would be an important additional tool to vascular and cardiac investigators.

Shandas and Zheng have recently developed an ultrasound based velocimetry technique, termed echo particle image velocimetry [18] (Echo PIV). Particle image velocimetry is a whole field noninvasive instantaneous flow field measurement technique. PIV is based on the direct determination of the two fundamental dimensions of the velocity: displacement and time. Tracer particles are usually used in PIV and regarded as an observable pattern that is tied to the fluid. The observed tracer patterns at two subsequent instances are considered as the input and output of the system, and the velocity field is inferred from the analysis of the input and output signals. The Echo PIV method consists of identifying and tracking a flow tracer (ultrasound contrast microbubbles) within a flow field, and computing local velocity vectors using a velocimetry algorithm. The ultrasound beam is scattered by the “contrast agent”,

This work was supported by Shenzhen-Hong Kong Innovation Circle Grant.

First author Lili Niu, is with Northeastern University, Sino-Dutch Biomedical and Information Engineering, Shenyang, China., and the Paul C. Lauterbur Research Center for Biomedical imaging, the Institute of Biomedical and Health Engineering, Shenzhen Institute of Advanced Technology, Chinese Academy of Sciences, Shenzhen, China 518067

Jing Wang, Ming Qian and corresponding author Hairong Zheng are with the Paul C. Lauterbur Research Center for Biomedical imaging, the Institute of Biomedical and Health Engineering, Shenzhen Institute of Advanced Technology, Chinese Academy of Sciences, Shenzhen, China 518067, and Key Laboratory of Biomedical Informatics and Health Engineering, Chinese Academy of Sciences, Shenzhen, China. (*e-mail: hr.zheng@siat.ac.cn).

microbubbles of gas surrounded by a lipid or protein sheath seeded into the fluid[18, 19]. Due to the huge acoustic impedance mismatch on the interface of bubble and fluid, the bubbles scatter strongly and “shine” acoustically in ultrasound field, resulting in a clear brightness mode image of the particle positions with excellent signal to noise ratio. Two sequential images (with time different between the two image frames determined by the system temporal resolution) are then subjected to Echo PIV analysis: the images are divided into interrogation windows and a cross-correlation between the two images gives the displacement of the particles, allowing a velocity vector field to be determined based on the time difference between the two images[20, 21].

This paper aims to optimize Echo PIV image processing method, so that processing accuracy would be enhanced. Sub-pixel calculation was utilized to maximize correlation accuracy and increase resultant spatial resolution. Then, this algorithm is employed in processing computer-generated particle image patterns and B-mode images of microbubbles in rotating flows.

II. EXPERIMENTAL SYSTEM

The general schematic of the Echo PIV system is shown in Fig.1(a). The Echo PIV system includes custom-designed PC controlled firing sequences, a novel 10MHz 128-element linear array transducer with element pitch of 0.46mm and bandwidth of 80%, RF data acquisition, B-mode image generation and a velocimetry algorithm for analyzing the RF-derived B-mode data (Figure 1(a)) [22]. The system was used to obtain real time velocity vectors within various mock carotid arteries. As shown in Figure 1(b), this Echo PIV system provides freedom in selecting several parameters: a much higher range of frame rates (up to 1000 s⁻¹) than available in commercial medical ultrasound systems, field of view (FOV) (15~60mm), number of transducer elements used to create ultrasound beams (1~128), imaging window width (4~38mm), focal depth (20~90mm) and power levels (MI: 0.2~1.2). Ultrasound contrast microbubbles (SF_6) are used as flow tracers and seeded into the flow.

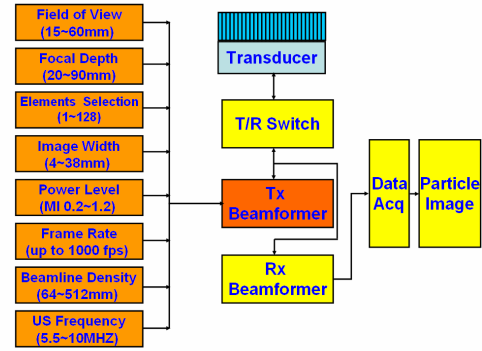
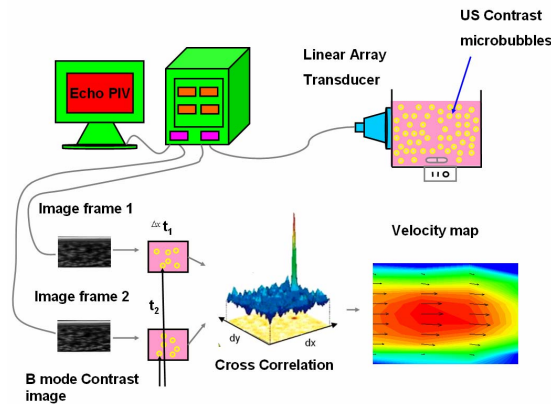


Figure 1. (a) Schematic of the custom-configured echo PIVsystem. (b) Transducer control interfaces, controllable parameters, and range of control values for each parameters.

III. EXPERIMENTAL METHOD

In the Echo PIV technique and system described above, two consecutive ultrasound contrast images are acquired by high frame rate ultrasound system and then subjected for particle pattern cross-correlation to obtain 2D initial velocity vectors. In most cases, pixels are integrates and the Echo PIV mainly deal with the pixels. The accuracy of Echo PIV will be affect if the actual length of pixel is not well measured.

After the image processing technology, sub-pixel technology can accurate to decimal precision pixel level [23]. This paper provides three formulas: (1) is peak centroid formula, (2) is parabolic peak fitting formula, (3) is Gaussian peak fitting formula [24-25].

$$(1) \begin{cases} \Delta x = i + \frac{(i-1)r_{pq}(i-1, j) + ir_{pq}(i, j) + (i+1)r_{pq}(i+1, j)}{r_{pq}(i-1, j) + r_{pq}(i, j) + r_{pq}(i+1, j)} \\ \Delta y = j + \frac{(j-1)r_{pq}(i, j-1) + jr_{pq}(i, j) + (j+1)r_{pq}(i, j+1)}{r_{pq}(i, j-1) + r_{pq}(i, j) + r_{pq}(i, j+1)} \end{cases}$$

$$(2) \begin{cases} \Delta x = i + \frac{r_{pq}(i-1, j) - r_{pq}(i+1, j)}{2r_{pq}(i-1, j) - 4r_{pq}(i, j) + 2r_{pq}(i+1, j)} \\ \Delta y = j + \frac{r_{pq}(i, j-1) - r_{pq}(i, j+1)}{2r_{pq}(i, j-1) - 4r_{pq}(i, j) + 2r_{pq}(i, j+1)} \end{cases}$$

$$(3) \begin{cases} \Delta x = i + \frac{\ln(r_{pq}(i-1, j)) - \ln(r_{pq}(i+1, j))}{2\ln(r_{pq}(i-1, j)) - 4\ln(r_{pq}(i, j)) + 2\ln(r_{pq}(i+1, j))} \\ \Delta y = j + \frac{\ln(r_{pq}(i, j-1)) - \ln(r_{pq}(i, j+1))}{2\ln(r_{pq}(i, j-1)) - 4\ln(r_{pq}(i, j)) + 2\ln(r_{pq}(i, j+1))} \end{cases}$$

$r_{pq}(i, j)$ is the maximum cross-correlation function. i and j are the corresponding coordinates when the cross-correlation function obtain the maximum value. $r_{pq}(i-1, j)$, $r_{pq}(i+1, j)$, $r_{pq}(i, j-1)$ and $r_{pq}(i, j+1)$ were cross-correlation functions around four nearest grid point. The three formulas can accurate to decimal

precision pixel level. In view of optimal property of the Gaussian function. This paper adopts Gaussian peak fitting formula.

The quantitative performance assessment made through synthetic Echo PIV images might yield order-of-magnitude improvement on the precision of the particle image displacement at a sub-pixel level when the image deformation is applied.

IV. RESULTS AND DISCUSSION

A. Simulation result

The sub-pixel processing algorithm was first studied in a computer simulated rotational flow field and particle image. Figure 2(a) is the simulation image of tracer particles (ultrasound contrast agent) at the t ; Figure 2(b) is the simulation picture of tracer particles (ultrasound contrast agent) at the $t + \Delta t$; Figure 3(a) shows the original velocity distribution obtained from Echo PIV processing. Pixels are integrates and the Echo PIV mainly deal with the pixels, so the accuracy of Echo PIV will be affected. After sub-pixel calculation was used, there is an obvious accuracy improvement by providing more finely flow vectors and velocity mapping result [figure 3(b)].

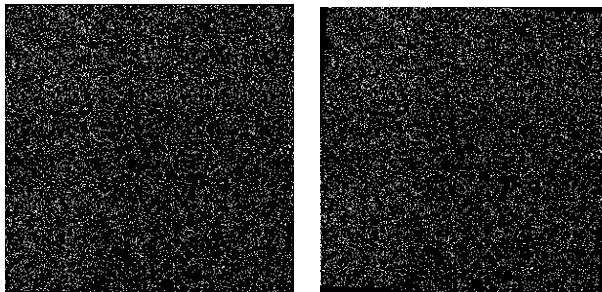


Figure 2: Simulation picture (a) the first particle image; (b) the second particle image.

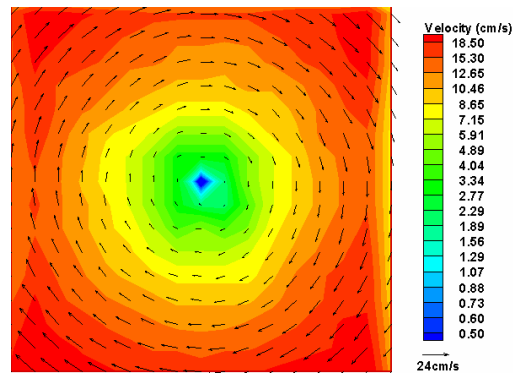
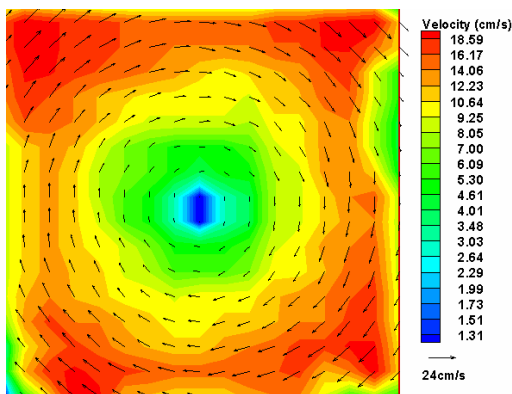


Figure 3: The velocity vectors and maps (a) The original velocity field measured by echo PIV; (b) velocity vectors were calculated by sub-pixel algorithm.

B. Experiment result

We also tested in the method in a rotational flow field on a high frame rate ultrasound imaging system. Figure 4 provides examples of such problems in an Echo PIV imaging of a rotating flow field. Figure 4(a) shows a portion of a B-mode image constructed from digital backscattered RF data of microbubbles within the rotation flow field. The particle images were obtained at a frame rate of 120 fps using 128 ultrasound beam lines with a focal depth of 8mm and field of view of 45mm. we used two iterative steps, from 64×64 to 32×32 pixel window size, with a 60% overlap and a cross-correlation was applied to the interrogation window over the entire imaging frame to determine the displacement of the particles and the resulting velocity field [figure 4(b)]. After sub-pixel calculation was used, there is good accuracy result [figure 4(c)].



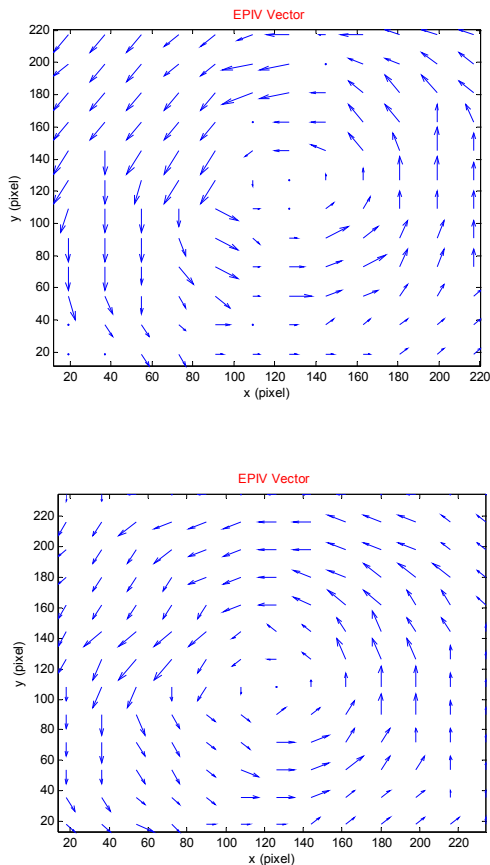


Figure 4: Rotating flow measurement (a) B-mode particle image of the flow; (b) The original velocity field measured by echo PIV; (c) velocity vectors were calculated by sub-pixel algorithm.

V. SUMMARY

In this paper, systemic sub-pixel calculation algorithm study on Post-Processing of Echo PIV imaging and velocimetry is implemented. Sub-pixel calculation algorithm was found to be able to maximize correlation accuracy and increase the imaging spatial resolution. Quantitative study on the imaging performance and accuracy improvement is still ongoing.

References

- [1] D. N. Ku, D. P. Giddens, D. J. Phillips, and D. E. Strandness, "Hemodynamics of the Normal Human Carotid Bifurcation - In vitro and In vivo Studies" *Ultrasound in Medicine and Biology*,11, 13-26, (1985).
- [2] M. H. Friedman, O. J. Deters, C. B. Barger, G. M. Hutchins, and F. F. Mark, "Shear-Dependent Thickening of the Human Arterial Intima" *Atherosclerosis*,60, 161-171, (1986).
- [3] R. M. Nerem, "Vascular Fluid-Mechanics, the Arterial-Wall, and Atherosclerosis" *Journal of Biomechanical Engineering Transactions of the Asme*,114, 274-282, (1992).
- [4] A. M. Malek, S. L. Alper, and S. Izumo, "Hemodynamic shear stress and its role in atherosclerosis" *Jama-Journal of the American Medical Association*,282, 2035-2042, (1999).
- [5] A. M. Shaaban and A. J. Duerinckx, "Wall shear stress and early atherosclerosis: A review" *American Journal of Roentgenology*,174, 1657-1665, (2000).
- [6] C. M. Gibson, L. Diaz, K. Kandarpa, F. M. Sacks, R. C. Pasternak, T. Sandor, C. Feldman, and P. H. Stone, "Relation of Vessel Wall

Shear-Stress to Atherosclerosis Progression in Human Coronary-Arteries" *Arteriosclerosis and Thrombosis*,13, 310-315, (1993).

- [7] S. Oyre, S. Ringgaard, S. Kozerke, W. P. Paaske, M. Erlandsen, P. Boesiger, and E. M. Pedersen, "Accurate noninvasive quantitation of blood flow, cross-sectional lumen vessel area and wall shear stress by three-dimensional paraboloid modeling of magnetic resonance imaging velocity data" *Journal of the American College of Cardiology*,32, 128-134, (1998).
- [8] Y. N. Jiang, K. Kohara, and K. Hiwada, "Association between risk factors for atherosclerosis and mechanical forces in carotid artery" *Stroke*,31, 2319-2324, (2000).
- [9] C. R. White, M. Haidekker, X. P. Bao, and J. A. Frangos, "Temporal gradients in shear, but not spatial gradients, stimulate endothelial cell proliferation" *Circulation*,103, 2508-2513, (2001).
- [10] Y. S. J. Li, J. H. Haga, and S. Chien, "Molecular basis of the effects of shear stress on vascular endothelial cells" *Journal of Biomechanics*,38, 1949-1971, (2005).
- [11] A. M. Malek, J. Zhang, J. W. Jiang, S. L. Alper, and S. Izumo, "Endothelin-1 gene suppression by shear stress: Pharmacological evaluation of the role of tyrosine kinase, intracellular calcium, cytoskeleton, and echanosensitive channels" *Journal of Molecular and Cellular Cardiology*,31, 387-399, (1999).
- [12] O. Traub and B. C. Berk, "Laminar shear stress: mechanisms by which endothelial cells transduce an atheroprotective force" *Arterioscler Thromb Vasc Biol*,18, 677-85, (1998).
- [13] D. A. Vorp, M. L. Raghavan, and M. W. Webster, "Mechanical wall stress in abdominal aortic aneurysm: Influence of diameter and asymmetry" *Journal of Vascular Surgery*,27, 632-639, (1998).
- [14] E. A. Finol and C. H. Amon, "Blood flow in abdominal aortic aneurysms: Pulsatile flow hemodynamics" *Journal of Biomechanical Engineering-Transactions of the ASME*,123, 474-484, (2001).
- [15] K. Hoshina, E. Sho, M. Sho, T. K. Nakahashi, and R. L. Dalman, "Wall shear stress and strain modulate experimental aneurysm cellularity" *Journal of Vascular Surgery*,37, 1067-1074, (2003).
- [16] C. L. Turner, S. Tebbs, P. Smielewski, and P. J. Kirkpatrick, "The influence of hemodynamic stress factors on intracranial aneurysm formation" *J Neurosurg*,95, 764-70, (2001).
- [17] R. A. Peattie, T. J. Riehle, and E. I. Bluth, "Pulsatile flow in fusiform models of abdominal aortic aneurysms: Flow fields, velocity patterns and flow-induced wall stresses" *Journal of Biomechanical Engineering-Transactions of the ASME*,126, 438-446, (2004).
- [18] H.R. Zheng, L.L. Liu, L.D.A. Williams, J.R.Hertzberg, Craig Lanning and R. Shandas. Real Time Multi-Component Echo Particle Image Velocimetry Technique For Opaque Flow Imaging. *Applied Physics Letters*. 88(26):261915, 2006.
- [19] J. R. Lindner, "Microbubbles in medical imaging: current applications and future directions" *Nature Reviews Drug Discovery*,3, 527-532, (2004).
- [20] J. E. Chomas, P. A. Dayton, D. May, J. Allen, A. Klivanov, and K. Ferrara, "Optical observation of contrast agent destruction" *Applied Physics Letters*,77, 1056-1058, (2000).
- [21] M. Gharib and D. Dabiri, An Overview of Digital Particle Image Velocimetry in Flow Visualization:Techniques and Examples. 2000, London: Imperial College Press.pp.
- [22] Yasuhiko Sugii, Shigeru Nishio, Taketoshiokuno, Kojiokamoto. A highly accurate iterative PIV technique using a gradient method [J], *Measurement Science and Technology*,11:1666-1673,(2000).
- [23] C. Morandi, F. Piazza and R. Capancioni, "Digital image registration by phase correlation between boundary maps", *IEE Proc.*, Vol. 134, pt. E, no. 2, pp. 101-104, Mar. 1987.
- [24] M.F. Erden, M.A. Kutay, and H.M. Ozaktas. Repeated filtering in consecutive fractional fourier domains and its application to signal restoration. *IEEE Trans. Signal Processing*, 47(5), 1999